World Journal of Engineering Research and Technology
WJERT
www.wjert.org
Impact Factor Value: 5.924

SYNTHESIS AND CHARACTERIZATION OF A KAOLIN-RICH CEMENT PRECURSOR OF A CONCRETE FOR DISPOSAL OF LOW-LEVEL RADIOACTIVE WASTE

Yasmina Mouheb, Nour-El-Hayet Kamel*, Soumia Kamariz, Fairouz Aouchiche and Dalila Moudir

Algiers Nuclear Research Center CRNA, Division of Environement, Safety and Nuclear Waste, 2. Bd Frantz Fanon, P.O.Box: 399, Alger-RP, Algiers, Algeria.

Article Received on 15/09/2020 **Article Revised on 05/10/2020** **Article Accepted on 26/10/2020**

***Corresponding Author**
Nour-El-Hayet Kamel
Algiers Nuclear Research Center CRNA, Division of Environement, Safety and Nuclear Waste, 2. Bd Frantz Fanon, P.O.Box: 399, Alger-RP, Algiers, Algeria.

ABSTRACT

Concrete is a second containment barrier for low-level radioactive elements. Cement-based materials are widely used in the nuclear industry for the packaging and storage of radioactive waste. Actually, innovative concretes contain cements with both Si_2O_5 and Si_2O_6 units in aluminosilicates. In this study, kaolin-enriched cement is synthesized from sand, gravel, Ca_2SiO_4 and $Ca_3Al_2O_5$. It is calcined at 1450°C for 2 h. Its structure is identified before incorporation into the concrete. The characterization of this cement is carried out by different methods of analysis XRD, FTIR, SEM. The X-ray diffraction analysis shows that this cement is mainly constituted by 90% $XAlSi_3O_8$ alkaline aluminosilicates (X can be K, Li or Na), with Si_2O_6 units. The Fourier Transform Infrared spectroscopy shows the main bonds vibrations of $KAlSi_3O_8$ and those of feldspars, such as the asymmetrical elongation vibrations of (Si–O–Si) and (Si–O–Al(Si)), the deformation absorption of (O–Si(Al)–O) and (O–Si–O). The shoulder between 1000 and 1200 cm^{-1} is associated to the stretching of Si(Al)-O tetrahedrons. These bands overlap with those of $LiAlSi_4O_{10}$ petalite, a secondary aluminosilicate phase in the cement, which contains Si_2O_5 units. The Scanning electron microscopy micrographs show the cement morphology. The aim of synthesizing cement with Si_2O_5 and Si_2O_6 units is reached.

KEYWORDS: Cement, aluminosilicates, Si_2O_5, Si_2O_6, low-level radioactive waste

I. INTRODUCTION

Low-level wastes are mainly generated from medical establishments, research centers and facilities using radioisotopes. For their diversity, the concrete and cement that must contain them must have a good durability to ensure the long-term storage of these wastes.

Cement-based materials are widely used in the packaging of low- and intermediate-level radioactive waste for the coating of these wastes in a primary container, which in turn can be wrapped in a secondary container (Glasser and Atkins, 1994).

In order to synthesize a new concrete that has many long-term sustainability properties, we are interested in the study of kaolin enriched cement. The kaolin clay replaces bentonite, which is frequently used in the composition of cements dedicated to low-level waste confinement concretes (Glasser and Atkins, 1994; Kwon et al., 2019; Moulin et al., 2001). The durability of such cement barriers and their interaction with the other materials are still widely discussed (Gaucher and Blanc, 2006; Blanc et al., 2010).

Concrete is a complex composite material made from aggregate agglomerated by a binder. Cement is a hydraulic binder. Tempered with water, it forms a cement paste that hardens by dissolving/precipitating reactions. After hardening, it exhibits both a satisfactory strength and stability (Kallel et al., 2009).

In this work, we are interested in the synthesis of kaolin-rich cement (Gaucher and Blanc, 2006), which will be used as an additive in a concrete for disposal of low-level radioactive wastes. We employed a kaolin rock containing kaolinite with the chemical formula $A1_2Si_2O_5(OH)_4$ and leaf structure, with a reticular distance of 7.5A°. The kaolin acts as a binder to improve the mechanical properties and hardness of the material. It has advantage of being very cheap and available in easily exploitable deposits (Saadi et al., 1993). Generally, raw natural kaolin contains other impurities such as quartz, feldspar, etc. (Zunino and Scrivener, 2020; Saikia et al., 2003).

The materials are synthesized by sintering at high temperature. The phases' identification is performed by X-ray diffraction (XRD) analysis. The material microstructure was revealed by both scanning electron microscopy (SEM) observations, and Fourier Transform Infrared Spectroscopy (FTIR).

II. MATERIAL AND METHODS

The reagents are used for the cement synthesis: 30 g of kaolin, 20 g $CaSO_4$ (tap regulator), 15g Ca_2SO_4, 15 g $Ca_3Al_2O_5$. A batch of 80g of mixture is prepared, and homogenized during 5 h. The cement is dried, decarbonized, and calcined at 1450°C for 3 hours in a BLF-1800 carbolite furnace, with the following thermal cycle: from room temperature to 500°C with a heating step of 10°/min, from 500 to 1450°C with a step of 6°/min. The product is removed from the furnace to stop any chemical reaction.

The cement XRD analysis is conducted by a Philips X'Pert PRO apparatus, operating at CuKα1 wavelength (λKα1 = 0.15406 nm). The analytical parameters were as follow: V = 40 kV and I = 40 mA; a 2θ scanning from 3° to 80°, with a scanning speed of 0.0701°/s. The XRD data are collected at room temperature on milled and sieved glass samples, with a mean size of 80 µm. For this, a 5657 Gmbh Retsch automatic agath mortar was used. The spectrum is identified using the Philips X'Pert plus 2004 software (Philips X'Pert High Score Package, 2004).

The material' microstructure is revealed by transversal sections SEM observations by a Philips XL30 microscope.

The cement FTIR spectrum is collected in the range of 400–4000 cm^{-1} using a Nicolet 380 FTIR spectrometer. The accuracy of this technique is estimated to be ±4 cm^{-1}. The FTIR spectra absorption measurements are performed using the KBr pellet technique at room temperature. The obtained spectrum is analyzed using OMNIC software.

III. RESULTS AND DISCUSSIONS

The sintered materials are grinded into fine powders (Figure 1) before characterization.

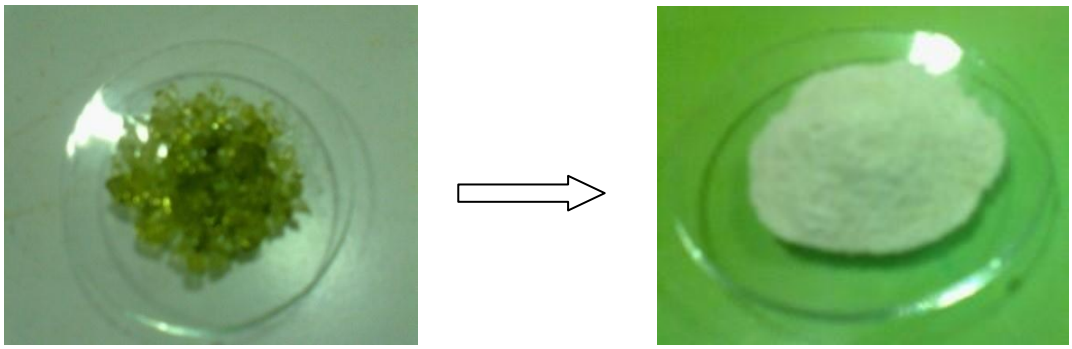

1.a. The cement before milling. **1.b. The milled cement.**

Figure 1: The synthesized cement before and after milling.

III.1. XRD phase's identification

The cement XRD spectrum is given in figure 2. The X'Pert High Score Plus phase identification of the cement reveals 90% of alkaline d'aluminosilicates, with the chemical formula: $XAlSi_3O_8$ (X can be K, Li or Na), with 25% of $KAlSi_3O_8$ (JCPDS 01-080-2108), 16% of $AlSi_3O_8$ (JCPDS 01-086-0098), 27% of albite $NaAlSi_3O_8$ (JCPDS 01-080-1094) and 22% of albite (JCPDS 01-076-0898). The remaining 10% is petalite $LiAlSi_4O_{10}$ (JCPDS 01-075-1716).

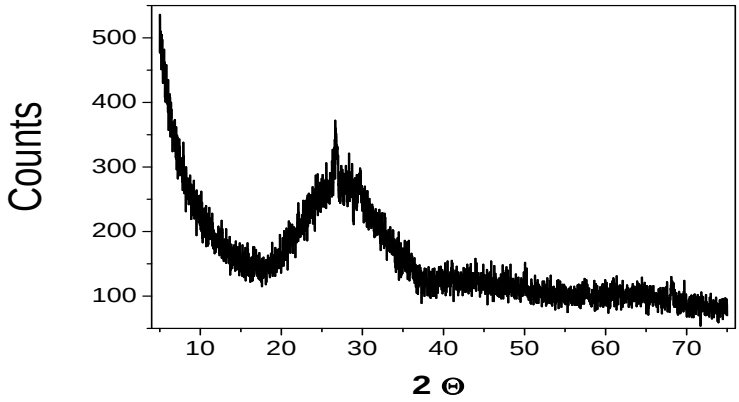

Figure 2: XRD Spectra of the synthesized cement.

III.2. Scanning electron microscopy

Typical SEM micrographs of this material are shown on Figure 3. The micrographs reflect the general structure of the minerals constituting the material. The grain structure is found to be elongated. According to Melo et al. (2001) kaolinite morphology is in the form of anhedric crystals (no euhedric faces) with elongated, rounded, or poorly defined forms.

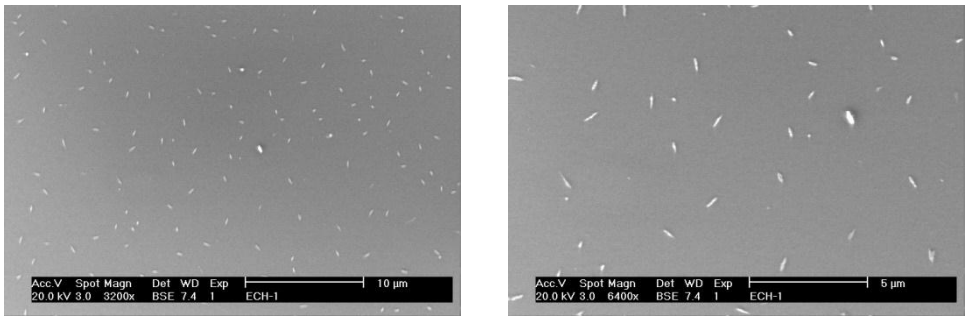

3.a. 3200x **3.b. 6400 x**

Figure 3: Typical SEM micrographs of the synthesized cement.

III.3. FTIR Analysis

The FTIR spectrum of kaolinite-based cement is given in Figure 4. It shows the main vibrations of the bonds of the $KAlSi_3O_8$ molecule and those of feldspars. Asymmetrical strain vibration bands as Si-O-Si and Si-O-Al(Si) are observed in the area 1200-1000 cm^{-1}.

Symmetric elongation occurs in the 800–500 cm^{-1} region. This region is sensitive to rearrangement of Si/Al. Before 500 cm^{-1}, there are the strain vibration absorption bands of (O–Si(Al)–O) and (O–Si–O) (Derivatograms, 1992). In regions 630–617cm^{-1} and 585–570 cm^{-1}, the $NaAlSi_3O_8$ – $CaAl_2Si_2O_8$ series appear, such as deformations (O–Si(Al)–O) and elongations (O–Si(Al)–O) and (O–Si–O). The shifts in this region are due to the high sensitivity of the arrangement and the structural order of Al and Si in tetrahedral sites, the elongation vibrations being in the region 800–500 cm^{-1} (Derivatograms, 1992). Between 650 and 530 cm^{-1}, we observe several maximums, the shoulder between 1000 and 1200 cm^{-1} is associated to the stretching of the Si(Al)-O tetrahedrons. These bands overlap with those of the petalite $LiAlSi_4O_{10}$ at 1075, 1016s, 780, 757, 734, 707, 470s, 435, and 420 cm^{-1} (Shukanov, 2014).

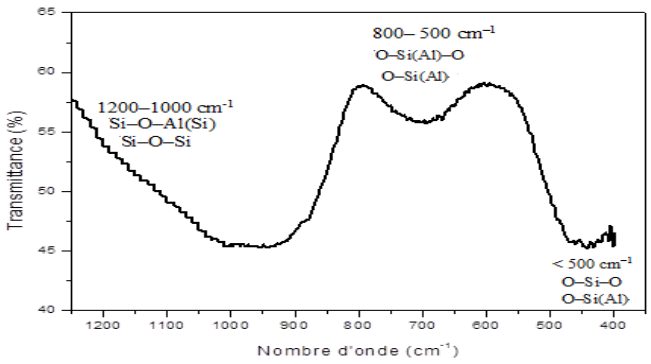

Area of 400-1200 cm^{-1}.

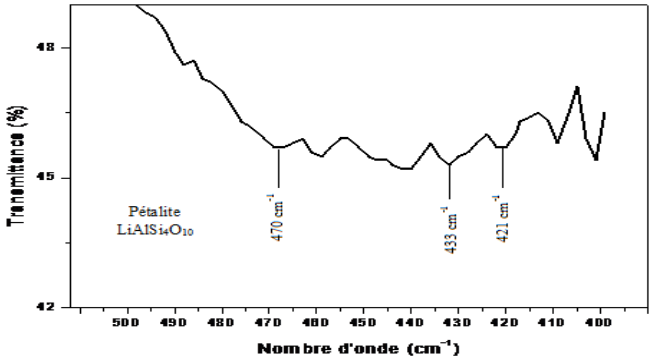

Area of 400-500 cm^{-1}

Figure 4: FTIR spectrum of kaolin-enriched cement.

IV. CONCLUSION

In this study, we have synthesized and characterized a kaolin-enriched cement. This material is intended to coat packages for disposal of low-level radioactive waste. The synthesis process is based on the calcination of the powder mixture at 1450°C with brutal cooling to stop any chemical reaction.

The XRD analysis shows that the cement contains 90% alkaline aluminosilicates: $XAlSi_3O_8$ (X can be K, Li or Na) and the remaining 10% are petalite $LiAlSi_4O_{10}$. FTIR and SEM analyses confirm the results obtained by XRD analysis. The aim of synthesizing cement with Si_2O_5 and Si_2O_6 units is reached.

V. REFERENCES

1. Blanc Ph, Bourbon X, Lassin A and Gaucher E C "Chemical model for cement-based materials: Temperature dependence of thermodynamic functions for nanocrystalline and crystalline C–S–H phases", Journal of Cement and Concrete Research, 2010; 40(6) : 851-866.
2. Derivatograms, Infrared Mössbauer Spectra of Standard Samples of Phase Composition. St. Petersburg, 1992.
3. Gaucher E C and Blanc P "Cement/clay interactions – A review: Experiments, natural analogues, and modeling", Waste Management, 2006; 26(7): 776-788.
4. Glasser F P and Atkins M. "Cements in Radioactive Waste Disposal", Journal of Materials Research Society Bulletin, 1994; 19(12): 33-38.
5. Kallel T, Samet B and Baklouti S ''Etude de l'interaction ciment-kaolin calciné en présence de lignosulfonate'', Silicates Industriels, 2009; 74(1): 321-329.
6. Kwon S, Hwang H and Lee Y "Effect of Pressure Treatment on the Specific Surface Area in Kaolin Group Minerals", Journal of Crystals, 2019; 9: 528-535.
7. Melo V F, Singh B, Schaefer C E G R, Novais R F and Fontes M P F "Division S-9— Soil Mineralogy: Chemical and Mineralogical Properties of Kaolinite-Rich Brazilian Soils", Soil Science Society American Journal, 2001; 65: 1324–1333.
8. Moulin E, Blanc P and Serrentino D "Influence of key cement chemical parameters on the properties of metakaolin blended cements", Cement and Concrete Composites, 2001; 23: 463-469.
9. Philips X'Pert High Score Package Diffraction Data CD-ROM, International Center for Diffraction Data, Newtown Square, 2004.

10. Saadi L, Jabry E, Moussa R and Gomina M "Etude des propriétés physico-chimiques et mécaniques de matériaux céramiques élaborés à partir d'une argile du Maroc : Partie I", Silicates Industriels, 1993; 3-4: 51- 57.
11. Saikia N J, Bharali D J, Sengupta P, Bordoloi D, Goswamee R L, Saikia P C, Borthakur P C "Characterization, beneficiation and utilization of a kaolinite clay from Assam, India", Applied Clay Science, 2003; 24: 93-103.
12. Shukanov N V Infrared spectra of mineral species V1, Springer Mineralogy, 2014.
13. Zunino F and Scrivener K "Increasing the kaolinite content of raw clays using particle classification techniques for use as supplementary cementitious materials", Journal of Construction and Building Materials, 2020; 244: 118335.